Proceedings of the International Gas Turbine Congress 2003 Tokyo
November 2-7, 2003

IGTC2003Tokyo TS-081

Effects of Rotation Speed on Heat Transfer in a 90°-Rib Roughened Two-Pass Duct

Yun Young Kim, Kyung Min Kim, Dong Ho Rhee and Hyung Hee Cho†

Department of Mechanical Engineering
Yonsei University
134 Shinchon-Dong, Seodaemun-Gu, Seoul 120-749, KOREA
Phone: +82-2-2123-2828, FAX: +82-2-312-2159, E-mail: hhcho@yonsei.ac.kr

ABSTRACT

The present study investigates the effects of rotation speed on heat/mass transfer characteristics in a 90°-rib roughened two-pass duct. The rotating duct has an aspect ratio (*W:H*) of 1:2 and a hydraulic diameter (D_h) of 26.67 mm. 90°-rib turbulators are installed on the leading and trailing side of the duct with a pitch-to-rib height ratio (p/e) of 10 and a rib height-to-hydraulic diameter ratio (e/D_h) of 0.056. Reynolds number based on the duct hydraulic diameter is constant at 10,000 and Rotation number ranges from 0.0 to 0.20. A naphthalene sublimation technique is employed to measure detailed local heat/mass transfer coefficients on the walls inside the duct. The results show that heat/mass transfer characteristics are dominated by secondary flows generated by the 180°-turn, rib turbulators, and duct rotation significantly. The turning region produces one pair of counter-rotating vortex cells. These vortices cause high heat/mass transfer in the turning region and in the upstream region of the second-pass. 90°-rib turbulators disturb main flow to generate reattachment and separation on ribbed surfaces and consequently enhance heat/mass transfer two times more. The rotation of duct induces Coriolis force that deflects main flow and results in differences on heat/mass transfer distributions between the leading and trailing surface. As Rotation number increases, the effects of duct rotation become more conspicuous. Discussions on flow and heat/mass transfer characteristics are presented describing how rotation speed changes the flow patterns and local heat transfer in the duct.

NOMENCLATURE

D_h	duct hydraulic diameter
D_{naph}	mass diffusion coefficient of naphthalene vapor in air, 0.681 (avg); Goldstein and Cho (1995)
e	rib height
H	duct height
h	heat transfer coefficient
h_m	mass transfer coefficient
$\dot{m}$	local naphthalene mass transfer rate per unit area
Nu	Nusselt number, hD_h / k
P_{naph}	naphthalene vapour pressure
p	rib-to-rib pitch
Pr	Prandtl number
$\dot{Q}_{air}$	volume flow rate of air
R	maximum radius of rotating arm
R_{naph}	gas constant of naphthalene
Re	Reynolds number, $D_h V / \nu$
Ro	Rotation number, $D_h \Omega / V$
Sc	Schmidt number, 2.28; Goldstein and Cho (1995)
Sh	Sherwood number, $h_m D_h / D_{naph}$
Sh_0	Sherwood number of a fully developed turbulent flow in a smooth pipe
$\overline{Sh}$	regional averaged Sherwood number
T_w	wall temperature
V	duct average bulk velocity without ribs
W	duct width
x	streamwise distance
y	lateral distance
z	height from naphthalene coated surface
$\overline{z_{sub}}$	lateral average naphthalene sublimation depth

Greek Symbols

Δt	runtime
Δz	sublimation depth of naphthalene surface
μ	dynamic viscosity
ν	kinematic viscosity
ρ_s	density of solid naphthalene
$\rho_{v,b}$	bulk vapor density of naphthalene
$\rho_{v,w}$	vapor density of naphthalene on the surface
Ω	angular velocity

INTRODUCTION

Internal passage cooling technique is widely adopted to protect modern advanced gas turbine blades exposed to high temperature combustion gases from thermal damages. By flowing coolant fluid from turbine compressors into passages located inside the blades, heat is removed from blade surfaces and thus blade materials do not exceed maximum allowable temperature. Moreover, designing turbine blades to stand high temperature is also essential to improve gas turbine performance because the turbine inlet temperature (TIT) largely determines the efficiency. Therefore, various researchers concentrated their work on the clarification of heat transfer mechanisms in internal cooling passages. It is reported that many factors related to the geometry of cooling passages and operating condition of turbine blades determine the efficiency of cooling performance. Among them, rib turbulators are one of the major fields of study. To enhance convection, various types of rib turbulators are installed on the surfaces of internal cooling passages. These rib turbulators disturb the coolant flow, break boundary layers, induce secondary flow patterns and finally promote heat

Manuscript Received on May 13, 2003

transfer in the cooling channels. Han et al. (1998) studied the effects of rib angle-of-attack and duct aspect ratio on the distribution of local heat transfer coefficient for developing flow in a one-pass duct. In their study, four different rib angle-of-attack (90°, 60°, 45° and 30°) and three different duct aspect ratio (1, 2 and 4) are employed. They reported that heat transfer increases after $x/D_h \geq 3$ due to the inducement of secondary flow when ribs are angled. Taslim et al. (1997) conducted heat transfer experiments with a ribbed low-aspect-ratio one-pass duct. From the results of twelve rib geometries, they concluded that high blockage ratio ribs were insensitive to the pitch-to-height ratio and that the performance decreased with the blockage ratios. Kiml et al. (1999) investigated heat transfer distribution and flow behavior in a one-pass duct. Four different angled-ribs are installed in a rectangular passage in parallel and staggered arrangements. They measured Nusselt number ratios in the duct and performed flow visualization, evaluating the result of each rib turbulators. Authors (Cho et al., 2000 and 2001; Lee et al., 2002) also studied the effects of rib turbulators in a one-pass duct. The influences of continuous full-ribs and discrete ribs on both heat/mass transfer and friction loss are clarified. Rib arrangements, the number of gaps and the length of discrete ribs were the main focus of authors' previous research.

When the internal cooling passages are composed of multi-channels, the bend, or turning region, produces vortex cells because centrifugal forces affect the main flow passing there and it results in high heat transfer, as have been reported by many authors. Liou et al. (1999) concentrated to understand the flow and heat transfer characteristics in the turning region. They specifically investigated the effects of divider thickness by using LDV (laser Doppler velocimetry) measurements and liquid crystal thermography. Mochizuki et al. (1999) performed heat transfer investigations in two-pass ducts with and without ribs. 90°- and 60°-rib turbulators are installed in four different arrangements and the effects on heat transfer are studied. They also conducted flow visualization in the 180°-turning region using paraffin mist and laser light source. The secondary flow pattern in the turn is captured in their research. Chen et al. (2000) also investigated detailed mass transfer distribution in a 90°-ribbed two-pass duct. They presented Sherwood number ratios along the centerline of the duct and explained the effect of the turning region on local Sherwood number distributions from the understanding of the secondary flow developed in the bend.

The rotation of blades - or internal cooling passages - causes different heat transfer phenomena. When the passages are rotating, Coriolis force and centrifugal buoyancy force appear and cause heat transfer discrepancy between the leading and trailing side of the blade deflecting the main flow of coolant fluid. Dutta et al. (1996) studied the local heat transfer in rotating smooth and ribbed two-pass square ducts. They concluded that rib turbulators, rotation and channel orientation change the characteristics of Nusselt number ratio distribution. Mochizuki et al. (1996) measured detailed Nusselt number ratios in ribbed two-pass ducts. Three different angled-ribs are used to understand how ribs affect the heat transfer coefficients in the rotating ducts. They reported that angled rib turbulators have more substantial effects on heat transfer enhancement than 90°-ribs do. Liou et al. (2001) performed TLCT(transient liquid crystal thermography) and LDV measurements in a rotating sharp turning duct. With the local distribution of heat transfer coefficients and analysis of flow field, they clarified the heat transfer and flow characteristics in their rotating duct. Morris et al. (1992), Bons et al. (1999) and Murata et al. (2001) studied the effect of centrifugal buoyancy force on the flow and heat transfer in rotating ducts. They explained how the centrifugal buoyancy force results in different heat transfer enhancement on the leading and trailing surface of the cooling passage. The previous studies of authors (Cho et al., 2002a, 2002b, 2002c and 2003) also investigated the heat/mass transfer characteristics in smooth and ribbed rotating ducts. The experimental studies covered the effects of various factors such as tip shape of divider walls, rib arrangements, rib turbulators, Reynolds numbers and Rotation numbers. Numerical studies by using a commercial package (Fluent 5) presented the flow field patterns in the ducts.

The main objective of the present study is to understand the heat/mass transfer in a rotating two-pass duct roughened with 90°-rib turbulators. Specifically, the effects of 90°-ribs and rotation speed on detailed heat/mass transfer characteristics inside the duct modeled after an internal cooling passage of a gas turbine blade are investigated. Authors applied a naphthalene sublimation technique to measure detailed heat/mass transfer coefficients from the analogy of heat and mass transfer. There are two main reasons why the mass transfer experiment is conducted instead of a heat transfer experiment: First, the distributions of local heat/mass transfer coefficients are important to observe heat transfer characteristics more completely. In addition, they are very helpful to understand flow patterns in the duct. Second, removing centrifugal buoyancy force by performing the naphthalene sublimation method relaxes the stiffness in understanding complex flow and heat transfer characteristics.

EXPERIMENTAL APPARATUS

A schematic of the experimental apparatus is present in Fig. 1. The rotating facility comprises a rotating system, a flow system and a measuring system. A 3HP-DC motor connected with a V-belt drives the rotating shaft and its rotation speed (RPM) is monitored by an optical tachometer attached near the axis of shaft. Room air flows from a blower to the test section through a heat exchanger that regulates the temperature of air and an orifice flowmeter that monitors the flowrate. A frequency inverter adjusts the blowing rate. These simulate the operating condition of gas turbine blades. Electrical output signals from the duct are recorded via slip rings using a Hewlett-Packard data logger interfaced to a computer. J-type thermocouples are put in both duct inlet and outlet, and also in the test plate to measure bulk air temperature and naphthalene surface temperature, respectively. An ice bath is used for thermocouple reference junction.

Figure 2 shows the test duct made of Plexiglas. The two-pass duct has a 180°-turning region. Its hydraulic diameter (D_h) is 26.67 mm and aspect ratio (W:H) is 1:2. Divider wall has thickness of 0.225 D_h with a round-shaped tip. The distance from the tip to outer wall of the turn is 0.75 D_h. Maximum rotating radius to the hydraulic diameter (R/D_h) is 21.63. 90°-rib turbulators are installed on the leading and trailing surfaces of the first- and second-pass.

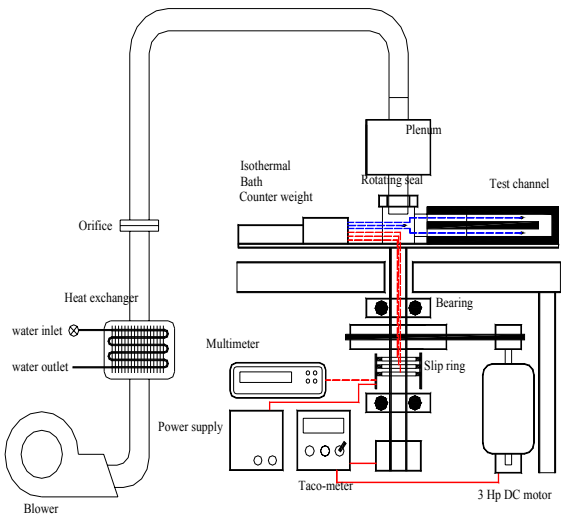

Fig. 1 A schematic diagram of the experimental apparatus

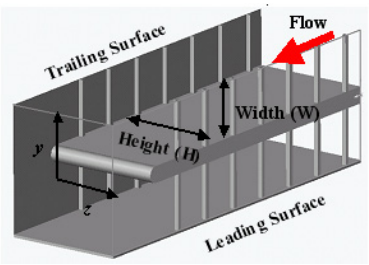

Fig. 2 Geometry of the 90°-rib roughened two-pass duct

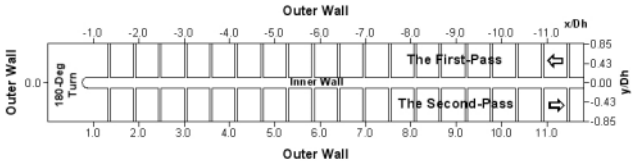

Fig. 3 The coordinate system

The height (e) and width of square ribs are both 1.5 mm. Pitch-to-rib height ratio (p/e) is 10 and rib height-to-hydraulic diameter ratio (e/D_h) is 0.056.

A naphthalene sublimation method is employed to measure detailed heat/mass transfer coefficients by using the analogy between heat and mass transfer. The inside walls of leading and trailing surfaces are coated with naphthalene, which simulate a cooling channel's two-sided heating condition of a gas turbine blade. This boundary condition of naphthalene-coated surfaces corresponds to a uniform wall temperature condition in heat transfer experiments, and that of inactive surfaces to an adiabatic wall condition. The temperature of naphthalene surface is accurately measured using J-type thermocouples installed in test plates since the vapor density of naphthalene is sensitive to temperature and varies approximately 10 percent per the temperature change of 1 °C.

The coordinate system is presented in Fig. 3. The streamwise, lateral and vertical direction corresponds to the axis of x, y, and z, respectively. The domain of mass transfer measurement covers in the mainstream direction along the outer wall of the duct from x/D_h=-11.815, which is the start point of the naphthalene surface in the first-pass, to x/D_h=11.815, the end point of the naphthalene surface in the second-pass, and x/D_h=0 corresponds to the middle of the turn. In the lateral direction the domain ranges from y/D_h=-0.85, which is the outer wall of the second-pass, to y/D_h=0.85, the outer wall of a first-pass. Experiments are performed for the fixed Reynolds number of 10,000 and for various Rotation numbers from 0.0 to 0.2 to investigate heat transfer characteristics of rotating gas turbine blades. The Rotation number of 0.2 corresponds approximately to 420 RPM with the present rotating facility.

DATA REDUCTION

The local mass transfer coefficient is obtained from the naphthalene sublimation depth, which is the difference of local surface depth on each position. By using a LVDT (Liner Variable Differential Transformer) and an automated positioning table, the sublimation depth is measured before and after the run of the duct experiments. The local mass transfer coefficient is obtained from calculation with the correction of the sublimation due to the natural convection during the measuring and installing/disassembling of the naphthalene-coated plate. It is expressed as

$$h_m = \frac{\dot{m}}{\rho_{v,w} - \rho_{v,b}} = \frac{\rho_s (\Delta z / \Delta t)}{\rho_{v,w} - \rho_{v,b}} \qquad (1)$$

where $\dot{m}$ is the local mass transfer rate of naphthalene per unit area which is determined from the density of solid naphthalene, ρ_s, and the sublimation rate, $\Delta z / \Delta t$. $\rho_{v,w}$ and $\rho_{v,b}$ are the vapor density of naphthalene on the surface and the bulk air, respectively. The former is calculated from the ideal gas law using the vapor pressure and the surface temperature as

$$\rho_{v,w} = \frac{P_{naph}}{R_{naph} T_w} \qquad (2)$$

The naphthalene vapor pressure, P_{naph}, is determined from the equations suggested by Ambrose et al. (1975). The latter, or the bulk vapor density of naphthalene, is obtained from the lateral average naphthalene sublimation depth, $\overline{z_{sub}}\big|_x$, measured at each position in the mainstream direction as

$$\rho_{v,b} = \frac{\rho_s W x}{\dot{Q}_{air} \Delta t} \overline{z_{sub}}\Big|_x \qquad (3)$$

From the local mass transfer coefficient, the Sherwood number is calculated as

$$\mathrm{Sh} = h_m D_h / D_{naph} \qquad (4)$$

where D_{naph} is the diffusion coefficient of naphthalene in air. The properties of naphthalene suggested by Ambrose et al. (1975) and Goldstein and Cho (1995) are used in the present study. The uncertainty in the Sherwood number is estimated to be within ±7.7% at a 95% confidence level by using the uncertainty estimation method of Kline and McClintock (1953). The uncertainty of the naphthalene properties such as naphthalene vapor pressure with ±6.4% error and diffusion coefficient with ±3.1% error are the most dominant in determining the uncertainty of Sherwood number.

Nusselt numbers can be obtained from the Sherwood numbers by the heat and mass transfer analogy correlated as $\mathrm{Nu/Sh=(Pr/Sc)^{0.4}}$ for turbulent flows. The mass transfer results are presented as the Sherwood number ratios, $\mathrm{Sh/Sh_0}$, to estimate the heat/mass transfer augmentation effectively, where $\mathrm{Sh_0}$ is the Sherwood number for a fully developed turbulent flow in a smooth circular tube correlated by McAdams (1942) and converted to mass transfer parameters as

$$\mathrm{Sh_0 = 0.023 Re^{0.8} Sc^{0.4}} \qquad (5)$$

Finally, The regional averaged Sherwood number, $\overline{\mathrm{Sh}}$, is calculated by the integration of the local Sherwood numbers weighted by pitch-to-pitch area.

RESULT AND DISCUSSION

1. Local heat/mass transfer

Figures 4(a) to 4(e) show local Sherwood number distributions for the 90°-ribbed duct. The 90°-rib turbulators generate reattachment and separation of the flow near ribbed surfaces and consequently enhance heat/mass transfer in the inter-rib region by breaking the boundary layer. However, relatively low heat/mass transfer regions are observed right behind ribs due to the recirculation of flow. Figure 4(a) shows these phenomena clearly. For the stationary case, the local Sherwood number distributions in the leading and trailing surface are almost the same because of the geometrical symmetry. It is known from the result that heat/mass transfer increases in the regions between the 90°-ribs of the first-pass because of aforementioned flow characteristics. In the turning region, a pair of counter rotating vortex cells named "Dean

vortices" is generated due to a rapid curvature and thus locally high Sherwood number ratios are obtained around the 90°- and 180°-outer side of the wall where the rotating vortices impinge. High heat/mass transfer is still observed after the turning region from the beginning to middle of the second-pass due to the remaining influence of Dean vortices. Especially in the region near the outer wall of the second-pass inlet ($1.0 \le x/D_h \le 3.0$ and $-0.85 \le x/D_h \le -0.43$), local Sherwood number ratios increase four to five times more. However, this effect of the 180°-turn decreases as the flow reaches the exit of the second-pass, so that the contour of Sherwood number ratios restores its shape shown in the first-pass.

When the duct rotates, the heat/mass transfer discrepancy between the leading and trailing surface occurs (Figs. 4(b) to 4(d)). In the first-pass, heat/mass transfer increases on the trailing surface and decreases on the leading surface due to the effect of Coriolis force. At a relatively lower rotation number (Ro=0.05) only small differences of heat/mass transfer are observed in the inter-rib regions, however, the discrepancy becomes more significant as the rotation number increases because the Coriolis force is strengthened. At the inlet of turning region ($x/D_h \approx -1.0$), the area around the divider wall on the leading surface shows relatively lower Sherwood numbers, but on the trailing surface the values are higher. It is believed that the effect of Coriolis force from the first-pass still affects the heat/mass transfer in this region. In the upstream of the second-pass ($1.0 \le x/D_h \le 4.0$), the combined influence of vortices produced in the first-pass and in the turning region dominates local heat/mass transfer distributions. On the leading surface, the high local Sherwood number ratios explained in the stationary case increase even more and the size of this region also expands. Meanwhile, the distribution on the trailing surface changes so that high Sherwood number ratios located near the outer wall moves toward the inner wall, or divider wall ($y/D_h \approx -0.2$), with the increase of rotation speed. As the flow proceeds toward the exit of the duct, Dean vortices diminish and the secondary flow by Coriolis force influences dominantly. Consequently, the heat/mass transfer discrepancy is observed again. Heat/mass transfer increases on the leading surface and decreases on the trailing surface in the second-pass because of the reversed direction of Coriolis force.

At the maximum rotation number (Ro=0.20), the difference of heat/mass transfer between the leading and trailing surface appears obviously in both the first- and the second-pass (Fig. 4(e)). In the first-pass, the heat/mass transfer distribution reveal that high Sherwood number ratios are found where the secondary flow by Coriolis force impinges, that is, near the outer and inner wall side of the leading surface ($y/D_h \approx 0.85$ and 0.0, respectively) and in the middle of the trailing surface ($y/D_h \approx 0.43$). This is consistent with the direction of the secondary flow by Coriolis force. In the turning region, the heat/mass transfer characteristics near the 90°- and 180°-outer side of the leading and trailing walls show similar trend mentioned in the above paragraphs, but it is more conspicuous in the present rotation speed. In the beginning of the second-pass, the distribution of high Sherwood number ratios appears near the outer wall side of the duct ($-0.85 \le y/D_h \le -0.43$) on the leading surface and near the inner wall side ($-0.43 \le y/D_h \le 0.0$) on the trailing surface, as observed at the previous rotation numbers. It is inferred that the combined effects of Coriolis force and Dean vortices on local distribution of heat/mass transfer coefficients culminate at the maximum rotation number (Ro=0.2). In the downstream region of the second-pass, the effect of Coriolis force is predominant so that the heat/mass transfer augmentation is perceived on the leading surface in the same way that appeared on the trailing surface in the first-pass. Likewise, lower local Sherwood number ratios are observed on the trailing surface with the similar distributions shown on the leading surface in the first-pass. This supports that the direction of Coriolis force is reversed in the second-pass.

2. Regional averaged Sherwood number ratios

Figures 5(a) to 5(e) present the regional averaged Sherwood

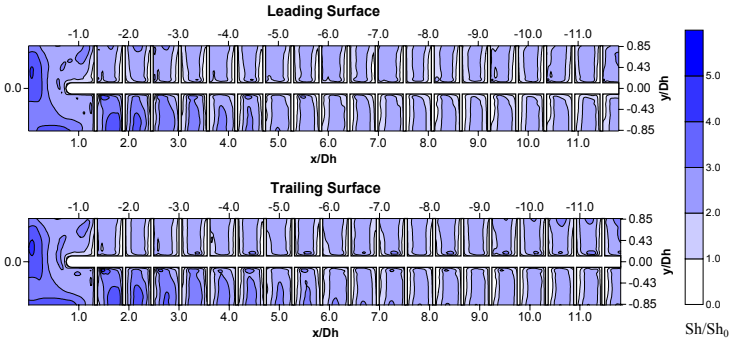

(a) Ro=0.0

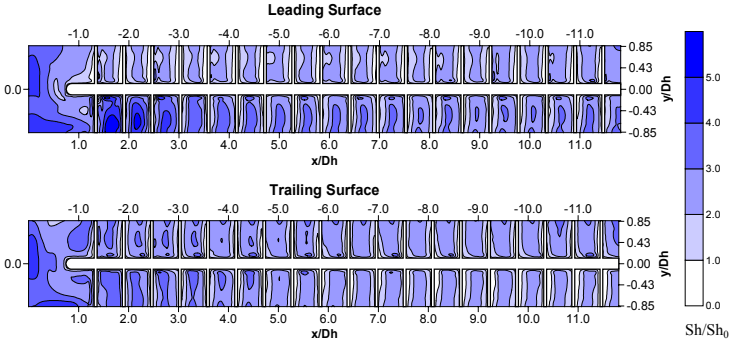

(b) Ro=0.05

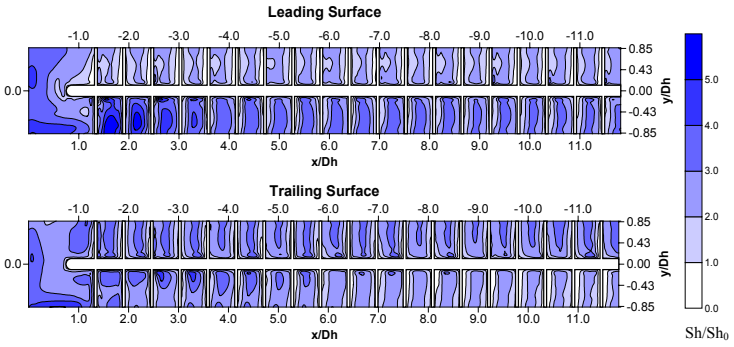

(c) Ro=0.10

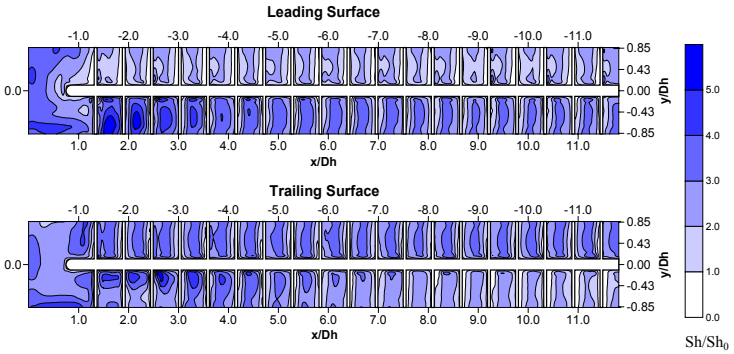

(d) Ro=0.15

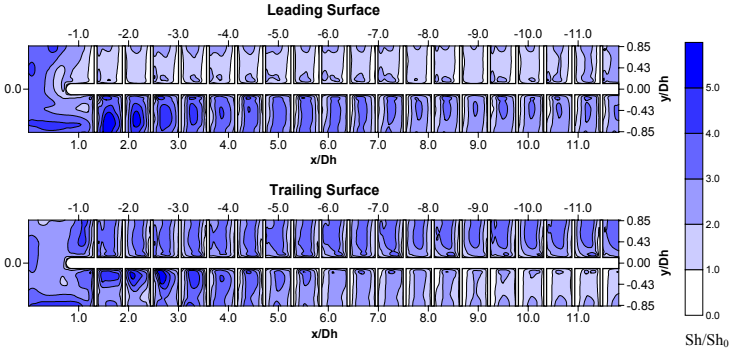

(e) Ro=0.20

Fig. 4 Sherwood number distributions for the 90°-ribbed duct

number ratios taken from the previous local coefficients for the 90°-ribbed duct. For the rotation number of 0.0, the average heat/mass transfer augmentation at the inlet of the first-pass is slightly higher, but it approaches to the value of $\overline{Sh}/Sh_0$=2.0 due to the development of flow (Fig. 5(a)). This means that the 90°-rib turbulators enhance heat/mass transfer approximately two times more when compared with a duct without rib turbulators, or a smooth duct. When the coolant fluid passes the 180°-turning region, Dean vortices are produced and thus the averaged Sherwood number ratios increase, having the peak value after the turning region (x/D_h≈1.6). The heat/mass transfer augmentation decreases in the second-pass as Dean vortices disappear due to rib turbulators and approaches to the fully developed value again.

With the rotation of duct, heat/mass transfer increases on the trailing surface and decreases on the leading surface in the first-pass due to the effect of the Coriolis force, as depicted in Figs. 5(b) to 5(d). The difference of heat/mass transfer becomes larger as the duct rotates faster. In the upstream of the second-pass, the combined effects of Coriolis force in the first-pass and the curvature in the turning region dominate the heat/mass transfer distributions, therefore the Sherwood number ratios increase on the leading surface and decrease on the trailing surface when compared with the result of stationary case (Fig. 5(a)). However, in the downstream of the second-pass, the heat/mass transfer discrepancy is shown again apparently resulting in the higher Sherwood number ratios on the leading surface and the lower in the trailing surface. This means that the Coriolis force has stronger influence on the flow and heat/mass transfer characteristics in the downstream of the second-pass than Dean vortices do. The direction of Coriolis force is reversed because the main flow is radially inward, and thus the flow is deflected toward the leading surface. Therefore, the regional averaged Sherwood number ratios are higher on the leading surface than those on the trailing surface near the outlet of the duct, as shown in Figs. 5(b) to 5(d).

At the highest rotation number (Ro=0.20), heat/mass transfer on the trailing surface is enhanced almost three times, whereas it does approximately 1.5 times only on the leading surface (Fig. 5(e)). In the upstream of the second-pass, the regional averaged Sherwood number ratios rise and fall down again as the coolant fluid proceeds to the exit of the duct due to the generation and diminishment of Dean vortices. It is believed from the heat/mass transfer result of the second-pass that the faster rotation speed causes to widen the discrepancy.

CONCLUSION

The present investigation focuses on the effects of rotation speed on heat/mass transfer in a 90°-rib roughened two-pass duct. Mass transfer experiments were performed to examine the effect of 90°-rib turbulators on heat/mass transfer augmentation on the leading and trailing surface of the duct. The effect of rotation speed was also studied by changing the Rotation number from 0.0 to 0.2, while keeping the duct Reynolds number constantly at 10,000. From the contour plots of local Sherwood number ratio (Sh/Sh_0) and the distributions of regional averaged Sherwood number ratios ($\overline{Sh}/Sh_0$), the main conclusions are led as follows:

(1) 90°-rib turbulators produce reattachment and separation of the flow near the ribbed surface and result in heat/mass transfer augmentation by breaking the boundary layer in inter-rib regions. For the stationary case (Ro=0.0), the heat/mass transfer increases two times more than that of the smooth duct.

(2) The 180°-turning region that connects the first-pass and the second-pass generates one pair of counter-rotating vortex cells, or the Dean vortices, due to sharp curvature and it dominates the heat/mass transfer characteristics in the turning region and the upstream of the second-pass. The peak value of Sherwood number ratios is observed after the turning region (x/D_h≈1.6).

(3) During duct rotation, the Coriolis force results in heat/mass transfer discrepancy between the leading and trailing surface.

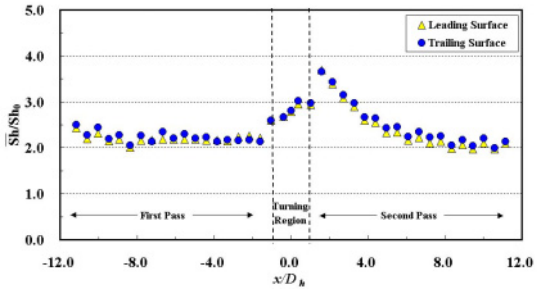

(a) Ro=0.0

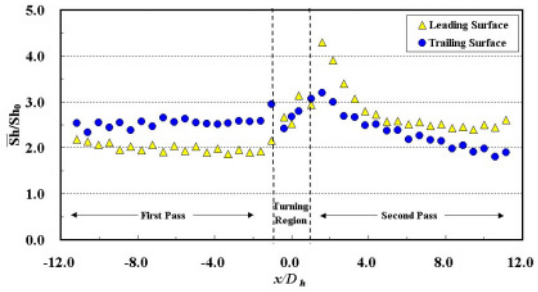

(b) Ro=0.05

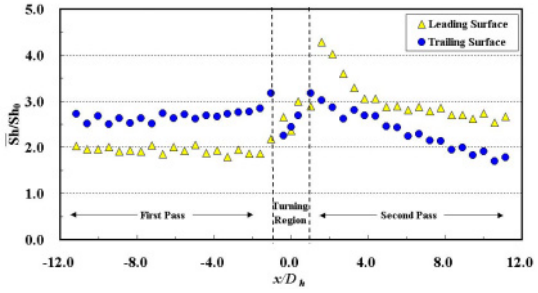

(c) Ro=0.10

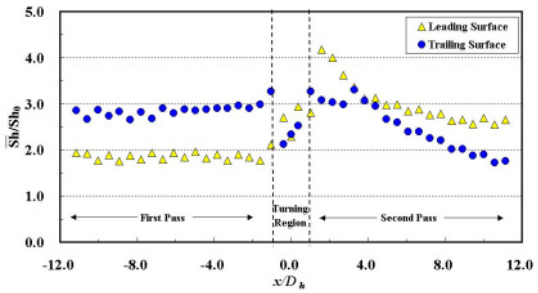

(d) Ro=0.15

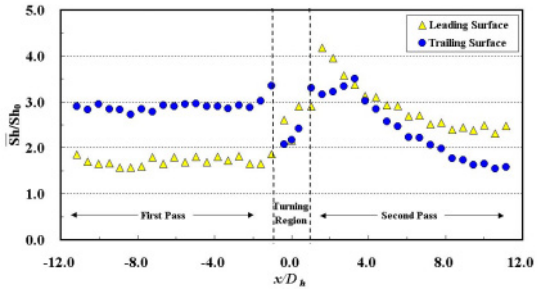

(e) Ro=0.20

Fig. 5 Regional averaged Sherwood number ratios for the 90°-ribbed duct.

Sherwood number ratios are higher on the trailing surface in the first-pass and on the leading surface in the second-pass. The characteristics of local heat/mass transfer coefficient

distributions depicted in contour plots of Sherwood number ratios are perceived apparently as the rotation speed increases.

(4) At the highest Rotation number (Ro=0.20), the effect of rotation culminates so that the widest difference of heat/mass transfer between the leading and trailing surfaces observed. Especially, the Sherwood number ratios in the first-pass triple on the trailing surface, whereas the ratios are enhanced approximately only 1.5 times on the leading surface.

ACKNOWLEDGMENT

This research was supported by Ministry of Science and Technology through their National Research Laboratory program.

REFERENCES

Ambrose, D., Lawrenson, I. J. and Sparke, C. H. S., 1975, "The Vapor Pressure of Naphthalene," *Journal of Chemical Thermodynamics*, Vol. 7, pp. 1173-1176.

Bons, J. P. and Kerrebrock, J. L., 1999, "Complementary Velocity and Heat Transfer Measurements in a Rotating Cooling Passage with Smooth Walls," *ASME Journal of Turbomachinery*, Vol. 121, pp. 651-662.

Chen, Y., Nikitopoulos, D. E., Hibbs, R., Acharya, S. and Myrum, T. A., 2000, "Detailed Mass Transfer Distribution in a Ribbed Coolant Passage with a 180° bend," *International Journal of Heat and Mass Transfer*, Vol. 43, pp.1479-1492.

Cho, H. H., Wu, S. J. and Kwon, H. J., 2000, "Local Heat/Mass Transfer Measurements in a Rectangular Duct with Discrete Ribs," *ASME Journal of Turbomachinery*, Vol. 122, pp. 579-586.

Cho, H. H., Lee, S. Y. and Wu, S. J., 2001, "The Combined Effects of Rib Arrangements and Discrete Ribs on Local Heat/Mass Transfer in a Square Duct," ASME Paper No. 2001-GT-0175.

Cho, H. H., Lee, S. Y., Rhee, D. H., Joo, W. G. and Lee, J., 2002a, "Effects of Rib Configuration on Heat/Mass Transfer in a Two-Pass Rotating Duct," *The 9th of International Symposium on Transport Phenomena and Dynamics of Rotating Machinery*, Paper No. HT-ABS-024.

Cho, H. H., Lee, S. Y. and Rhee, D. H., 2002b, "Heat Transfer in a Two-Pass Rotating Rectangular Duct with and without 70°-Angle Ribs," *Heat and Mass Transfer* (accepted).

Cho, H. H., Lee, S. Y. and Rhee, D. H., 2002c, "Effects of Cross Ribs on Local Heat/Mass Transfer in a Two-Pass Rotating Duct," *Heat and Mass Transfer* (accepted).

Cho, H. H., Kim, Y. Y., Kim, K. M. and Rhee, D. H., 2003, "Effects of Rib Arrangements and Rotation Speed on Heat Transfer in a Two-Pass Duct," ASME Paper No. GT-2003-38609.

Dutta, S. and Han, J. -C., 1996, "Local Heat Transfer in Rotating Smooth ad Ribbed Two-Pass Square Channels with Three Channel Orientations," *ASME Journal of Heat Transfer*, Vol. 118, pp. 578-584.

Goldstein, R. J. and Cho, H. H., 1995, "A Review of Mass Transfer Measurements Using Naphthalene Sublimation," *Experimental Thermal and Fluid Science*, Vol. 10, pp. 416-434.

Han, J. C. and Park, J. S., 1988, "Developing Heat Transfer in Rectangular Channels with Rib Turbulators," *International Journal of Heat Mass Transfer*, Vol. 31, No. 1, pp. 183-195.

Kiml, R., Mochizuki, S., Murata, A. and Nozicka, J., 1999, "Heat Transfer Distribution and Flow Behavior in a Rectangular Rib-Roughened Passage for the Parallel and Staggered Rib Arrangements," *Proceedings of the International Gas Turbine Congress 1999 Kobe*, pp. 857-863.

Kline, S. J. and McClintock, F. A., 1953, "Describing Uncertainty in Single-Sample Experiments," Mechanical Engineering, Vol. 75, pp. 3-8.

Lee, S. Y., Wu, S. J., Rhee, D. H., Choi, C., Kim, Y. Y. and Cho, H. H., 2002, "Local Heat/Mass Transfer Characteristics in a Square Duct with Various Rib Arrangements," *The 12th International Heat Transfer Conference*, pp. 117-122

Liou, T. -M., Tzeng, Y. -Y. and Chen, C. -C., 1999, "Fluid Flow in a 180 Deg Sharp Turning Duct with Different Divider Thickness," *ASME Journal of Turbomachinery*, Vol. 121, pp. 569-576.

Liou, T. -M., Chen, C. -C. and Chen, M. -Y., 2001, "TLCT and LDV Measurements of Heat Transfer and Fluid Flow in a Rotating Sharp Turning Duct," *International Journal of Heat and Mass Transfer*, Vol. 44, pp. 1777-1787.

McAdams, W. H., 1942, Heat Transmission, 2nd ed., McGraw-Hill, New York.

Mochizuki, S., Beier, M., Murata, A., Okamura, T. and Hashidate, Y., 1996, "Detailed Measurement of Convective Heat Transfer in Rotating Two-Pass Rib-Roughened Coolant Channels," *1996 ASME Turbo Asia Conference*, Paper No. 96-TA-6.

Mochizuki, S., Murata, A., Shibata, R. and Yang, W. -J., 1999, "Detailed Measurements of Local Heat Transfer Coefficients in Turbulent Flow Through Smooth and Rib-Roughened Serpentine Passages with a 180° Sharp Bend," *International Journal of Heat and Mass Transfer*, Vol. 42, pp. 1925-1934.

Morris, W. D. and Salemi, R., 1992, "An Attempt to Uncouple the Effect of Coriolis and Buoyancy Forces Experimentally on Heat Transfer in Smooth Circular Tubes Tat Rotate in the Orthogonal Mode," *ASME Journal of Turbomachinery*, Vol. 114, pp. 858-864.

Murata, A. and Mochizuki, S., 2001, "Effect of Centrifugal Buoyancy on Turbulent Heat Transfer in an Orthogonally Rotating Square Duct with Transverse or Angled Rib Turbulators," *International Journal of Heat and Mass Transfer*, Vol. 44, pp. 2739-2750.

Taslim, M. E. and Korotky, G. J., 1997, "Low-Aspect-Ratio Rib Heat Transfer Coefficient Measurements in a Square Channel," *International Gas Turbine and Aeroengine Congress and Exhibition*, Paper No. 97-GT-388.